Magnetic transition in $K_4Cu_4OCl_{10}$: A model system of three-dimensional spin-$\frac{1}{2}$ tetrahedra

Masayoshi Fujihala,[1] Xu-Guang Zheng,[1,2,*] Hiroki Morodomi,[3] Tatsuya Kawae,[3] and Isao Watanabe[4]
[1]*Department of Physics, Graduate School of Science and Engineering, Saga University, Saga 840-8502, Japan*
[2]*Department of Physics, Faculty of Science and Engineering, Saga University, Saga 840-8502, Japan*
[3]*Department of Applied Quantum Physics, Faculty of Engineering, Kyushu University, Fukuoka 819-0395, Japan*
[4]*RIKEN Nishina Center for Accelerator-Based Science, 2-1 Hirosawa, Wako, Saitama 351-0198, Japan*
(Received 27 December 2012; revised manuscript received 11 April 2013; published 30 April 2013)

Isolated spin tetrahedral systems with weak intertetrahedral couplings, as have been reported for $Cu_2Te_2O_5X_2$ (X = Cl, Br) and the related compound $Cu_4Te_5O_{12}Cl_4$, have received much attention recently because they represent an interesting class of magnets that consist of weakly coupled magnetic clusters and, in particular, they can directly demonstrate the interplay of intertetrahedral couplings with built-in tetrahedral frustration. However, there is much debate about the structural low dimensionality of the Cu-Te-O-Cl(Br) compounds and its effect on the magnetism of the material. Here, we present a model spin tetrahedral system $K_4Cu_4OCl_{10}$, with almost isotropic magnetic coupling within the tetrahedron and three-dimensional connection of the tetrahedra. The system enters a spin-singlet state with a susceptibility maximum at $T_{max} = 11$ K, and then enters an antiferromagnetic order at $T_N = 4.4$ K. The ratio $T_N/T_{max} = 0.40$ is close to the $T_N/T_{max} = 0.38$ for $Cu_2Te_2O_5Br_2$, which is viewed as an indicator of closeness to quantum criticality. Evidence in muon-spin rotation or relaxation suggests an incommensurate ordering. This work shows that the previously revealed ground state in anisotropically structured $Cu_2Te_2O_5X_2$ compounds also exists in an isotropic spin tetrahedral system.

DOI: 10.1103/PhysRevB.87.144425 PACS number(s): 75.10.Jm, 75.10.Kt, 75.25.−j

The magnetic phases of geometrically frustrated magnets have been rigorously researched both theoretically and experimentally over the last two decades. Geometric frustration, which results from an intrinsic incompatibility between fundamental magnetic interactions and the underlying lattice geometry (triangular, tetrahedral, or kagome lattices), gives rise to intriguing fundamental phenomena such as the formation of exotic states like spin ices, spin liquids, and magnetic monopoles.[1–3] Among them, the $S = \frac{1}{2}$ quantum spin systems, and in particular those consisting of Cu^{2+} spins, have received intense attention since Anderson suggested that a spin-$\frac{1}{2}$ Heisenberg antiferromagnet on the triangular lattice would have a gapless spin-liquid ground state, called a resonating-valence-bond state[4] and which is thought to be relevant to high-temperature superconductivity.[5]

While many of the kagome and pyrochlore antiferromagnets, which are much more complicated to model theoretically than the triangular lattice, are still not well understood, the isolated spin tetrahedral system with weak intertetrahedral coupling has received intense attention recently because it can directly demonstrate the interplay of intertetrahedral coupling with the built-in tetrahedral frustration. Of wider interest, they also represent an interesting class of magnets consisting of weakly coupled magnetic clusters. To date, the $Cu_2Te_2O_5X_2$ (X = Cl, Br) family and the related compound $Cu_4Te_5O_{12}Cl_4$ have been considered the only real systems of such tetrahedra, but they have remarkable structural anisotropies both inside and outside of the tetrahedra, thus leading to much controversy about their anisotropic magnetic coupling and dimensionality.[6–25] Among them, a spin-singlet state directly resulting from the intratetrahedral couplings forms at $T \sim$ 20–30 K. At lower temperatures, they exhibit unconventional magnetic instability and incommensurate order below $T_N = 18.2$ K in $Cu_2Te_2O_5Cl_2$ and $T_N = 11.4$ K in $Cu_2Te_2O_5Br_2$.[7,13,19] From the spin-topology point of view, the arrangement of Cu^{2+} satisfies all the prerequisites for quantum criticality. The unconventional magnetic instability and incommensurate ordering were interpreted to indicate that their quantum state is close to quantum criticality as a result of the competing intra- and intertetrahedral couplings. However, there are several open questions that raise a lot of discussion. The most important question is the magnetic dimensionality of the system due to the notable structural anisotropies inside and between the tetrahedra. As shown in Fig. 1(a) for $Cu_2Te_2O_5X_2$, there are obvious anisotropies in their crystal structure: the intratetrahedral Cu^{2+}–Cu^{2+} bonds have quite different bond lengths with different bonding anions, and magnetic coupling inside the tetrahedron was considered nearly isotropic due to stronger coupling along the longer bonds.[6] Nevertheless, the tetrahedra align along the c-axis direction with a notable one-dimensional chain feature. Therefore, it is of high interest to find whether a true three-dimensional system of coupled-spin tetrahedra also shows a similar magnetism. Here, we present such a model material: $K_4Cu_4OCl_{10}$, and report the magnetism of three-dimensional coupled-spin tetrahedra.

$K_4Cu_4OCl_{10}$ was labeled as the mineral Ponomarevite by de Boer *et al.,* in 1972.[26] We tried to synthesize it and finally succeeded in preparing pure-phase polycrystalline $K_4Cu_4OCl_{10}$ by using a low-temperature molten-salt reaction process. High-purity KCl, CuO, and $CuCl_2$ powders were mixed with the molar ratio of 4 : 1 : 3 and vacuum sealed into a quartz tube. The mixture was heated at 400 °C for two days and then slowly cooled. The crystal structure of the obtained polycrystalline sample was examined and determined by x-ray diffraction. The unit-cell parameters were refined using the Rietveld method with program REITAN-FP.[27] Magnetic susceptibility measurements were performed using a commercial superconducting quantum interference device magnetometer (MPMS; Quantum Design). The heat capacity was measured using an adiabatic heat-pulse method

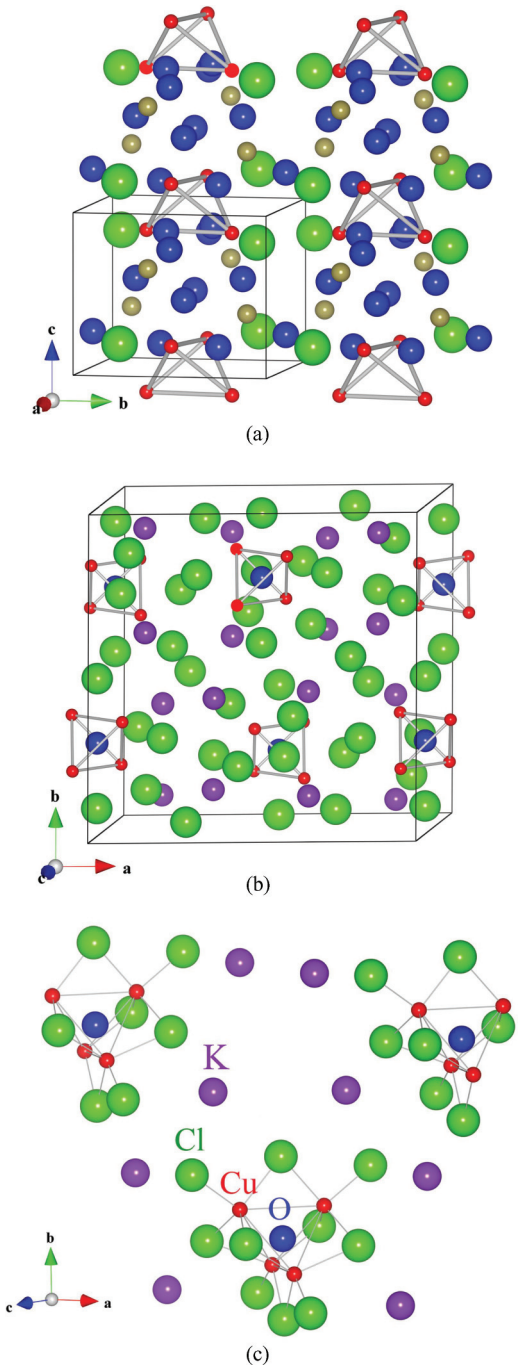

FIG. 1. (Color online) Crystal structures of spin tetrahedral systems of (a) $Cu_2Te_2O_5Cl_2$ and (b) $K_4Cu_4OCl_{10}$. Ions are represented by colored balls, with red for Cu^{2+}, blue for O^{-2}, green for halogen ions, and gray and purple for Te^{4+} and K^+, respectively. In panel (c) the local environment for the Cu^{2+} spins is illustrated more clearly.

with a ^{3}He cryostat using approximately one gram of the polycrystalline sample mixed with gold powder. A muon-spin rotation and relaxation (μSR) experiment was carried out using a spin-polarized single-pulsed surface-muon (μ^+) beam at the RIKEN-RAL Muon Facility at Rutherford Appleton Laboratory in the United Kingdom. A ^{3}He cryostat was used for temperature control. Furthermore, in order to check possible missing signals, the μSR spectra was verified using the dc continuous muon beam facility at the M15 port of the meson facility of TRIUMF in Canada.

The synthesized $K_4Cu_4OCl_{10}$ is single phase with a monoclinic crystal structure in space group $C\,2/c$. It has lattice parameters of $a = 14.74$ Å, $b = 14.90$ Å, $c = 8.948$ Å, and $\beta = 104.79°$. The results are in good consistency with those reported for Ponomarevite ($a = 14.70$ Å, $b = 14.88$ Å, $c = 8.95$ Å, and $\beta = 104.74°$).[26] As illustrated in Fig. 1(b), magnetic ions of Cu^{2+} form isolated spin tetrahedra. Compared to the large distortion of 11% to 12% in the $Cu_2Te_2O_5X_2$ system, the distortion of the tetrahedron is only 1.3% with the longest Cu^{2+}–Cu^{2+} distance being 3.15 Å and the shortest being 3.11 Å inside the tetrahedron. As illustrated in Fig. 1(c), the four Cu^{2+} spins on the corners of one tetrahedron are bonded to each other through the O at the center of the tetrahedron and Cl outside the tetrahedron. Therefore, superexchange interactions through them are considered to contribute to intratetrahedron magnetic coupling. Each Cu^{2+} is surrounded by four nearest Cl ions (at a distance of around 2.3 Å) and one O (at a distance of 1.91 Å). The average intertetrahedral distance is 6.472 Å, which is much longer than the 4.163–4.385 Å in the $Cu_2Te_2O_5X_2$ system. While the tetrahedra in $Cu_2Te_2O_5X_2$ are directly connected by the O and halogen ions, those in $K_4Cu_4OCl_{10}$ are connected through indirect Cl–K–Cl bonding, as shown in Fig. 1(c). Therefore, the above features would definitely lead to a weak intertetrahedral magnetic coupling. Another prominent and important feature of the present structure is the three-dimensional connection of the tetrahedra, which is strikingly different from the notable one-dimensional-chain feature in the $Cu_2Te_2O_5X_2$ system. Therefore, $K_4Cu_4OCl_{10}$ can be viewed as a model weakly coupled spin-$\frac{1}{2}$ tetrahedral system.

The temperature dependence of the magnetic susceptibility, $\chi = M/H$, is a maximum around $T_{\chi\,\mathrm{max}} = 11$ K and has a small kink at $T_N = 4.4$ K, as shown in Fig. 2 and the inset. The broad anomaly at $T_{\chi\,\mathrm{max}}$ resembles that of the $Cu_2Te_2O_5X_2$ and $Cu_4Te_5O_{12}Cl_4$ compounds,[7,24] wherein it was attributed to the presence of the singlet-triplet spin gap[6,7] and was consistently fit by using theoretical calculations for noninteracting spin tetrahedra. However, as shown in Fig. 2, the susceptibility of $K_4Cu_4OCl_{10}$ could not be well fit by the equation for noninteracting spin tetrahedra that was defined in Ref. 6 or that was theoretically calculated for tetrahedron clusters.[16] This is considered to be caused by the influence of the intertetrahedral coupling. Here, we temporarily use a combined formula by adding a Curie-Weiss formula to the noninteracting spin tetrahedral equation as defined in Ref. 6, producing a seemingly intratetrahedral $J_1 = J_2 = 28$ K, and $\theta_{CW} = -29$ K with effective moment $\mu_{eff} = 1.48\mu_B/Cu^{2+}$, where θ_{CW} reflects intertetrahedral coupling. The fitted parameters, and especially the supposed Curie-Weiss temperature θ_{CW}, varied with the temperature range of the data used for fitting. For reference, we also show the fit using the data for $T > 50$ K to a single function of the Curie-Weiss formula in Fig. 2, which produced $\theta_{CW} = -31$ K and $\mu_{eff} = 1.78\mu_B$ (for $T > 100$ K, $\theta_{CW} = -27$ K, and $\mu_{eff} = 1.72\mu_B$). Obviously, more precise theoretical modeling for weakly interacting spin tetrahedra is needed. It is not clear why the effect of intertetrahedral coupling on the susceptibility was absent in the results of Ref. 6. The temperature $T_N = 4.4$ K in

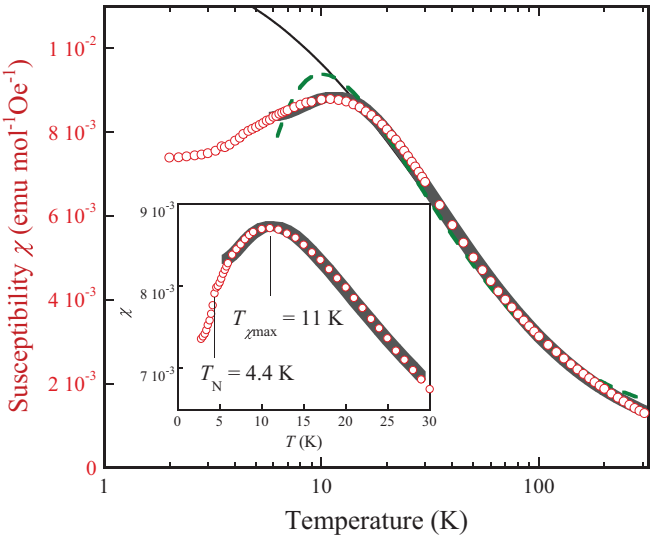

FIG. 2. (Color online) Temperature dependence of magnetic susceptibility χ per mol Cu measured at 1 T for $K_4Cu_4OCl_{10}$. The thick dashed line is a curve fit for noninteracting spin tetrahedra and the thick gray line is that containing a Curie-Weiss component, as described in the text (data at temperatures above 6 K are used for fitting). For reference, a curve fit (thin solid line) using the data above 50 K to the Curie-Weiss formula is also plotted. The inset shows an enlarged plot of the low-temperature part.

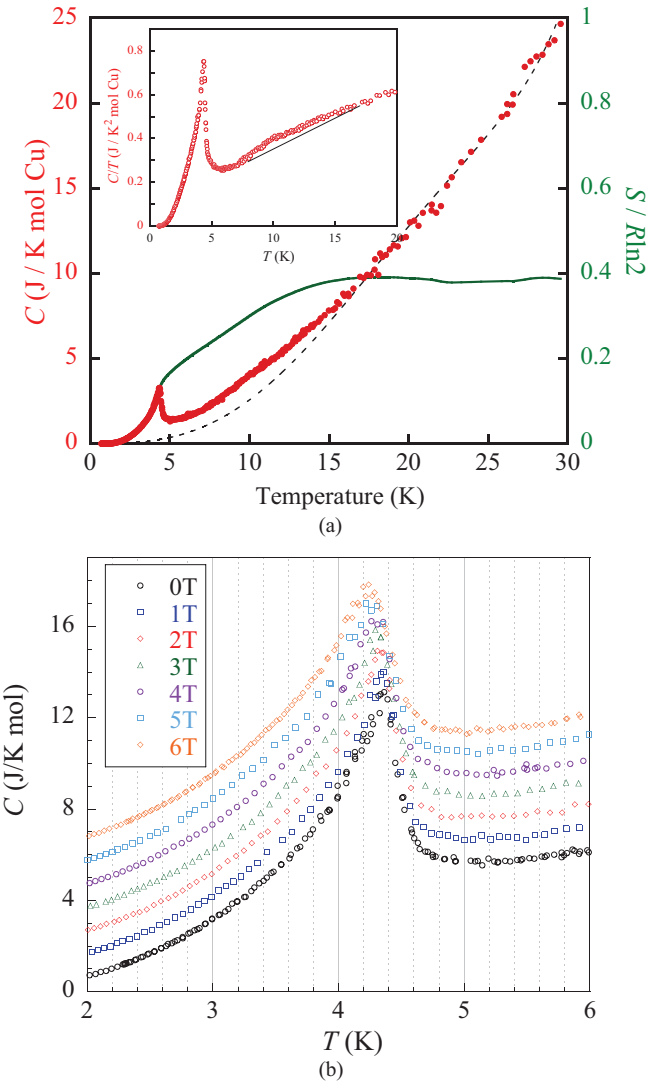

FIG. 3. (Color online) (a) Specific heat per mol formula for $K_4Cu_4OCl_{10}$ (left axis) and the roughly estimated magnetic entropy (solid line, right axis). The dashed line is an assumed lattice contribution to the specific heat. The inset plot shows the zero-field C/T depicting the broad anomaly around 11 K; the thin line is to guide to eyes to help to see the small, broad anomaly. (b) Specific-heat data under external fields showing the decrease of T_N with increasing field. The specific-heat data are shifted upward to clearly show the T_N decrease.

$K_4Cu_4OCl_{10}$ is much lower than that in the CuTe compounds, reflecting the much weaker intertetrahedral coupling.

More evidence of the presence of the spin-singlet state and antiferromagnetic transition is given by the specific heat. As shown in Fig. 3(a) and its inset, a sharp transition occurs at $T_N = 4.4$ K. The specific-heat curve shows a pronounced λ-shaped peak, which indicates the existence of a second-order phase transition. A small and broad feature is also verified around 11 K, supporting the spin-singlet state. As shown in Fig. 3(b), the transition at $T_N = 4.4$ K slightly decreased in external fields with $\Delta T_N/\Delta H = -0.021$ K/T, which is similar to $Cu_2Te_2O_5Cl_2$.[7] The lattice contribution deviated from the Debye law, which is not unusual for powder materials. An exact estimation of the magnetic entropy is difficult, especially because there is apparently a broad magnetic background around 11 K. An exact estimation could only be made by using a nonmagnetic reference compound. Therefore, we use the high-temperature parts of the specific-heat results, as shown in Fig. 3(a), to roughly estimate the magnetic specific heat and the magnetic entropy. The magnetic entropy is $0.39R\ln 2$ per spin, which is close to the $0.36R\ln 2$ per spin in $Cu_2Te_2O_5Cl_2$.[7]

We further utilized μSR studies to clarify whether the magnetic order below $T_N = 4.4$ K is incommensurate as for $Cu_2Te_2O_5X_2$. The positive muon μ^+ is a sensitive local probe for spin order and fluctuations. The time evolution of muon-spin asymmetry directly reflects the magnetic order and spin fluctuations.[28] A μSR study was carried out for a spin-tetrahedral system. Figure 4 shows the zero-field muon-spin asymmetry spectra of the $K_4Cu_4OCl_{10}$ at typical temperatures. No anomaly is observed around 11 K, supporting the absence of short-range correlation and the spin-singlet picture. The spectra for $T > 4.4$ K are best fit by a stretched exponential function,

$$a(t) = \exp[-(\lambda t)^{\beta}], \quad (1)$$

with an average value of $\lambda = 0.125(4)$ and $\beta = 1.72(3)$. The stretched exponential relaxation is verified to be caused by nuclear dipolar fields, which are suspected to be due to the nuclear spins of ^{35}Cl, ^{37}Cl, ^{35}Cu, ^{37}Cu, and ^{39}K in $K_4Cu_4OCl_{10}$. Apparently, the combined effect of these multiple nuclear dipolar fields leads to a phenomenologically described relaxation function of the stretched exponential. The field distribution is approximately $\Delta = \lambda/\gamma_\mu = 1.5$ G, which is typical for a nuclear dipolar field of Cl nuclei, suggesting that the positive muons stop in the vicinity of Cl^- ions. For $T < T_N$, muon-spin precessions with two distinct frequencies

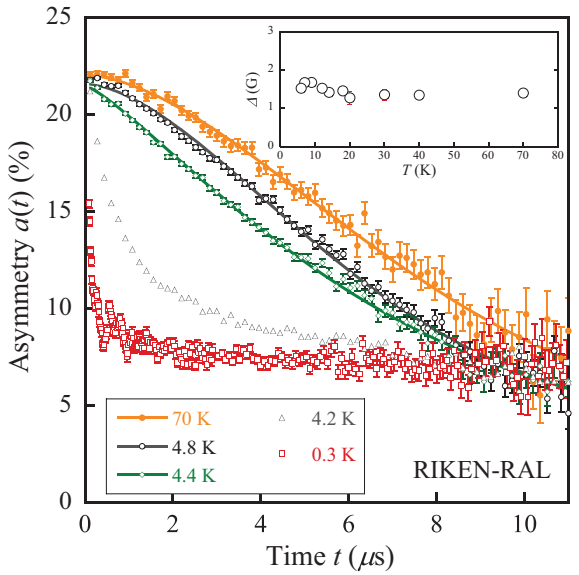

FIG. 4. (Color online) Zero-field μSR asymmetry spectra at typical temperatures for $K_4Cu_4OCl_{10}$ obtained from the RIKEN-RAL beam line. The solid lines on the back of high-temperature data are curves fits as described in the text. The inset shows the estimated nuclear field distribution Δ.

were clearly observed [e.g., the $T = 0.3$ K asymmetry spectra in Fig. 4 and a Fourier transform of the asymmetry spectra in Fig. 5], which unambiguously demonstrates the presence of long-range magnetic order. The experiment using the dc continuous beam facility at TRIUMF confirms that there are no missing frequencies. The muon precession frequencies and hence the local field are relatively small for the Cu^{2+} spin. This is due to the relatively long distance between the Cu^{2+} spin and the muon stopping site near the Cl^- ions [refer to the structure in Fig. 1(c)]. As viewed from the crystal structure, basically the Cl^- ions are located in two kinds of positions: one lying close to the tetrahedron and the other far, thus producing two precession frequencies for each ordered spin.

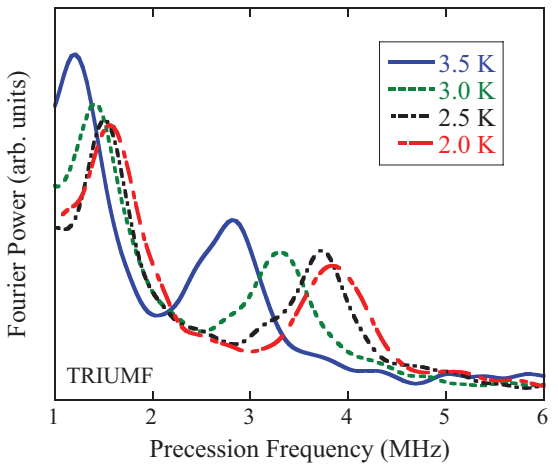

FIG. 5. (Color online) Fourier transform of asymmetry spectra showing broad-peak features of the muon spin precession frequencies in $K_4Cu_4OCl_{10}$.

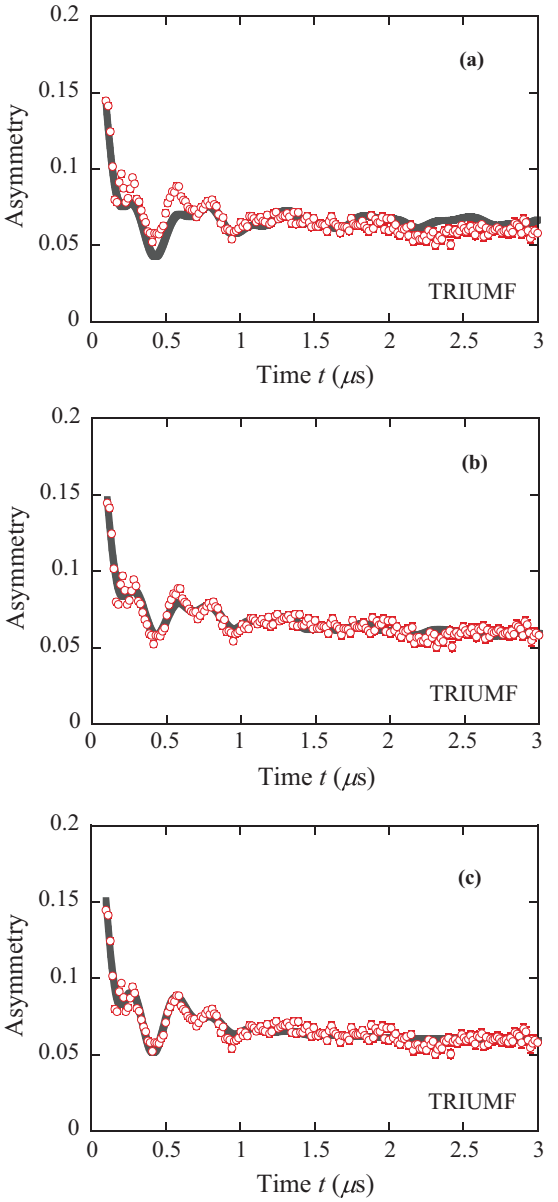

FIG. 6. (Color online) Examples of curve fits (thick line) using (a) a zero-order Bessel function and (b) a modified Bessel function as defined in Eq. (3) and (c) Eq. (4) for a fictitious commensurate order for the zero-field μSR asymmetry spectrum at 2 K (TRIUMF).

However, the muon-spin precession frequencies showed broad-peak features, as shown in Fig. 5, implying a broad field distribution produced by the ordered spins at muon-stopping sites in $K_4Cu_4OCl_{10}$. Consistent with the field distribution, the zero-field spectra as shown in Fig. 4 show a quick damping with time. These results contradict the usual Néel order and can be reasonably attributed to an incommensurate magnetic order. It is well established that, for incommensurate spatially inhomogeneous fields with a spread between 0 and H_{max},[29] the asymmetry for two-muon stopping sites is

$$a^{\mathrm{ICM}}(t) = \sum_{i=1}^{i=2} a_0^i \left[\frac{2}{3} j_0\left(\gamma_\mu H_{\max}^i t\right) + \frac{1}{3}\right], \qquad (2)$$

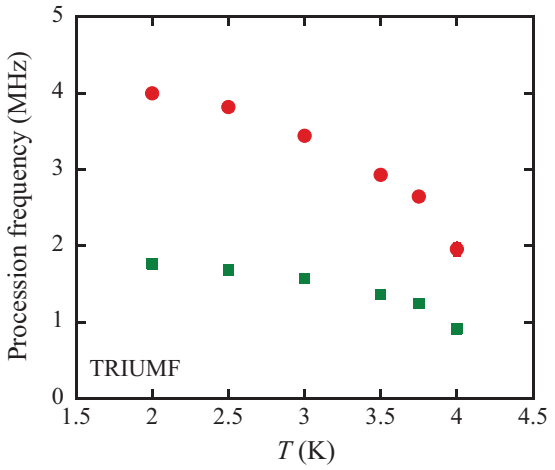

FIG. 7. (Color online) Temperature dependence of muon spin procession frequencies in $K_4Cu_4OCl_{10}$.

where j_0 denotes the spherical Bessel function, and $\gamma_\mu/(2\pi) = 13.55$ kHz/G is the muon gyromagnetic ratio. The damping of the Bessel function, reflecting the distribution of internal fields between 0 and H_{max}, is too strong and cannot completely account for our experimental spectra [Fig. 6(a)]. Similar situations occurred in other practical incommensurate systems (see, e.g., Refs. 30–33). This is expected since muons are coupled to the incommensurately ordered Cu^{2+} moments through a dipolar field; therefore, a narrower field distribution between H_{min} and H_{max} should be considered at each muon site, hence making the damping weaker. Unfortunately, exact muon stopping sites in $K_4Cu_4OCl_{10}$ are not known, so we could not calculate exact field distributions. A much better fit was obtained using a modified Bessel function [Fig. 6(b)], which is widely used for practical incommensurate systems,[31–33]

$$a^{\mathrm{ICM}}(t) = \sum_{i=1}^{i=2} a_0^i \left[\frac{2}{3} j_0\left(\gamma_\mu H_{\max}^i t\right) e^{-\lambda_1 t} + \frac{1}{3} e^{-\lambda_2 t}\right]. \quad (3)$$

Similar to that reported for $FeTe_2O_5Br$ in Ref. 30, an alternative fitting could be done using the function for a fictitious commensurate order,

$$a^{\mathrm{CM}}(t) = \sum_{i=1}^{i=2} a_0^i \left[\frac{2}{3} \cos(\gamma_\mu H^i t) e^{-\lambda_T t} + \frac{1}{3} e^{-\lambda_L t}\right]. \quad (4)$$

The model above accounts for relaxation at two-muon sites in a fictitious commensurate magnetic phase with well-defined oscillation frequencies $\gamma_\mu H^i$. Additional longitudinal and transverse relaxation rates λ_L and λ_T, respectively, are added. The latter can effectively serve to mimic the effect of the field distributions in the incommensurate phase, not affecting the modeled precession frequencies. As can be seen in Fig. 6(c), this model describes the experimental spectra reasonably well.

In Fig. 7 we plot the temperature dependence of the muon spin precession frequencies. Therefore, the μSR experiment strongly suggests an incommensurate magnetic order in $K_4Cu_4OCl_{10}$.

The present results are reasonable and interesting as compared to the known spin tetrahedral systems $Cu_2Te_2O_5X_2$. In $Cu_2Te_2O_5X_2$ and in special $Cu_2Te_2O_5Br_2$, a unconventional low-temperature incommensurate order has been suggested to be close to quantum criticality, reflecting the interplay of competing intratetrahedral and intertetrahedral couplings.[7–15,18–25] There have been a lot of arguments about the structural low dimensionality and the influence on magnetism in the Cu-Te-O-Cl(Br) compounds. For example, an inelastic-neutron investigation suggested the presence of low-dimensional correlations above T_N in $Cu_2Te_2O_5Br_2$.[17] The ratio of T_N versus the temperature of susceptibility maximum, $T_N/T_{\chi\,max}$, is viewed as an indicator of the closeness to the quantum criticality (e.g., in Refs. 7 and 24). The ratios $T_N/T_{\chi\,max}$ are 0.79, 0.72, and 0.38 for $Cu_2Te_2O_5Cl_2$, $Cu_4Te_5O_{12}Cl_4$, and $Cu_2Te_2O_5Br_2$, respectively. The ratio $T_N/T_{\chi\,max} = 0.40$ of $K_4Cu_4OCl_{10}$ is close to that of $Cu_2Te_2O_5Br_2$. The present work shows that the previously proposed ground state for structurally anisotropic $Cu_2Te_2O_5X_2$ compounds is also valid in an isotropic spin tetrahedral system.

In summary, we have presented a unique real material $K_4Cu_4OCl_{10}$ as an ideal isotropic spin tetrahedral system. The spin-singlet state, which was previously revealed for structurally chain-featured tetrahedral $Cu_2Te_2O_5X_2$ (X = Cl, Br), also exists in $K_4Cu_4OCl_{10}$. Unconventional incommensurate ordering has been reported for $Cu_2Te_2O_5Br_2$, indicating close-to-quantum-criticality states for spin tetrahedral systems. Here, our work shows that similar incommensurate ordering also exists in a three-dimensional isolated spin tetrahedral system.

This work is supported by a Grant-in-Aid for Scientific Research on Priority Areas to X.G.Z. (Grant No. 22014008) from The Ministry of Education, Culture, Sports, Science and Technology (MEXT). The μSR experiment is supported by the RIKEN Nishina Center for Accelerator-Based Science. We are grateful to Dr. Ikuto Kawasaki and Mr. Hanjie Guo at RIKEN Nishina Center for Accelerator-Based Science for technical assistance in the μSR experiment. We are also grateful to Bassam Hitti, Donald Arseneau, and Syd Kreitzman at TRIUMF, Canada, for their continuing technical support for the μSR experiments at TRIUMF.

*zheng@cc.saga-u.ac.jp

[1] S. T. Bramwell and M. J. P. Gingras, Science **294**, 1495 (2001).
[2] L. Balents, Nature (London) **464**, 199 (2010).
[3] C. Castelnovo, R. Moessner, and S. L. Sondhi, Nature (London) **451**, 42 (2008).
[4] P. W. Anderson, Mater. Res. Bull. **8**, 153 (1973).
[5] P. W. Anderson, Science **235**, 1196 (1985).
[6] M. Johnsson, K. W. Törnroos, F. Mila, and P. Millet, Chem. Mater. **12**, 2853 (2000).
[7] P. Lemmens, K.-Y. Choi, E. E. Kaul, C. Geibel, K. Becker, W. Brenig, R. Valenti, C. Gros, M. Johnsson, P. Millet, and F. Mila, Phys. Rev. Lett. **87**, 227201 (2001).

[8]K. Totsuka and H.-J. Mikeska, Phys. Rev. B **66**, 054435 (2002).
[9]Wolfram Brenig, Phys. Rev. B **67**, 064402 (2003).
[10]Roser Valentí, T. Saha-Dasgupta, Claudius Gros, and H. Rosner, Phys. Rev. B **67**, 245110 (2003).
[11]C. Gros, P. Lemmens, M. Vojta, R. Valentí, K.-Y. Choi, H. Kageyama, Z. Hiroi, N. V. Mushnikov, T. Goto, M. Johnsson, and P. Millet, Phys. Rev. B **67**, 174405 (2003).
[12]A. V. Sologubenko, R. Dell'Amore, H. R. Ott, and P. Millet, Eur. Phys. J. B **42**, 549 (2004).
[13]O. Zaharko, A. Daoud-Aladine, S. Streule, J. Mesot, P.-J. Brown, and H. Berger, Phys. Rev. Lett. **93**, 217206 (2004).
[14]Valeri N. Kotov, Michael E. Zhitomirsky, Maged Elhajal, and Frédéric Mila, Phys. Rev. B **70**, 214401 (2004).
[15]M. Prester, A. Smontara, I. Živković, A. Bilušić, D. Drobac, H. Berger, and F. Bussy, Phys. Rev. B **69**, 180401(R) (2004).
[16]J. T. Haraldsen, T. Barnes, and J. L. Musfeldt, Phys. Rev. B **71**, 064403 (2005).
[17]S. J. Crowe, S. Majumdar, M. R. Lees, D. McK. Paul, R. I. Bewley, S. J. Levett, and C. Ritter, Phys. Rev. B **71**, 224430 (2005).
[18]O. Zaharko, H. Rønnow, J. Mesot, S. J. Crowe, P. J. Brown, A. Daoud-Aladine, A. Meents, A. Wagner, M. Prester, H. Berger, and D. M. Paul, Phys. Rev. B **73**, 064422 (2006).
[19]Z. Jagličić, S. ElShawish, A. Jeromen, A. Bilušić, A. Smontara, Z. Trontelj, J. Bonča, J. Dolinšek, and H. Berger, Phys. Rev. B **73**, 214408 (2006).
[20]Jens Jensen, Phys. Rev. B **79**, 014406 (2009).
[21]Kwang-Yong Choi, Hiroyuki Nojiri, Naresh S. Dalal, Helmuth Berger, Wolfram Brenig, and Peter Lemmens, Phys. Rev. B **79**, 024416 (2009).
[22]A. Comment, H. Mayaffre, V. Mitrović, M. Horvatić, C. Berthier, B. Grenier, and P. Millet, Phys. Rev. B **82**, 214416 (2010).
[23]X. Wang, K. Syassen, M. Johnsson, R. Moessner, K.-Y. Choi, and P. Lemmens, Phys. Rev. B **83**, 134403 (2011).
[24]Rie Takagi, Mats Johnsson, Vladimir Gnezdilov, Reinhard K. Kremer, Wolfram Brenig, and Peter Lemmens, Phys. Rev. B **74**, 014413 (2006).
[25]Badiur Rahaman, Harald O. Jeschke, Roser Valentí, and T. Saha-Dasgupta, Phys. Rev. B **75**, 024404 (2007).
[26]J. J. de Boer, D. Bright, and J. N. Helle, Acta Crystallogr. Sect. B **28**, 11 (1972).
[27]F. Izumi and K. Momma, Solid State Phenom. **130**, 15 (2007).
[28]Alain Yaouanc and Pierre Dalmas de Reotier, *Muon Spin Rotation, Relaxation, and Resonance: Applications to Condensed Matter* (Oxford University Press, Oxford, 2010).
[29]M. Science, in *Muons in Physics, Chemistry, and Materials*, edited by S. L. Lee, S. H. Kilcoyne, and R. Cywinski (Taylor & Francis, Abingdon, 1999).
[30]A. Zorko, M. Pregelj, H. Berger, and D. Arčon, J. Appl. Phys. **107**, 09D906 (2010).
[31]J. Sugiyama, Y. Ikedo, K. Mukai, J. H. Brewer, E. J. Ansaldo, G. D. Morris, K. H. Chow, H. Yoshida, and Z. Hiroi, Phys. Rev. B **73**, 224437 (2006).
[32]Y. Ikedo, J. Sugiyama, H. Nozaki, H. Itahara, J. H. Brewer, E. J. Ansaldo, G. D. Morris, D. Andreica, and A. Amato, Phys. Rev. B **75**, 054424 (2007).
[33]Y. J. Uemura, A. A. Aczel, Y. Ajiro, J. P. Carlo, T. Goko, D. A. Goldfeld, A. Kitada, G. M. Luke, G. J. MacDougall, I. G. Mihailescu, J. A. Rodriguez, P. L. Russo, Y. Tsujimoto, C. R. Wiebe, T. J. Williams, T. Yamamoto, K. Yoshimura, and H. Kageyama, Phys. Rev. B **80**, 174408 (2009).